MIT Open Access Articles

Enhancement of Thermoelectric Properties by Modulation-Doping in Silicon Germanium Alloy Nanocomposites

Enhancement of thermoelectric properties by modulation-doping in silicon germanium alloy nanocomposites

Bo Yu[1,§], Mona Zebarjadi[2,§], Hui Wang[1], Kevin Lukas[1], Hengzhi Wang[1], Dezhi Wang[1], Cyril Opeil[1], Mildred Dresselhaus[3], Gang Chen[2,*], and Zhifeng Ren[1,*]

[1] Department of Physics, Boston College, Chestnut Hill, Massachusetts 02467, USA

[2] Department of Mechanical Engineering, Massachusetts Institute of Technology, Cambridge, Massachusetts 02139, USA

[3] Department of Physics and Department of Electrical Engineering and Computer Science, Massachusetts Institute of Technology, Cambridge, Massachusetts 02139, USA

[§] These authors contributed equally to this work

[*] To whom the correspondence should be addressed: gchen2@mit.edu, renzh@bc.edu

Abstract:

Modulation-doping was theoretically proposed and experimentally proved to be effective in increasing the power factor of nanocomposites $(Si_{80}Ge_{20})_{70}(Si_{100}B_5)_{30}$ by increasing the carrier mobility, but not the figure-of-merit (*ZT*) due to the increased thermal conductivity. Here we report an alternative materials design, using alloy $Si_{70}Ge_{30}$ instead of Si as the nanoparticles and $Si_{95}Ge_5$ as the matrix, to increase the power factor but not the thermal conductivity, for achieving a *ZT* of 1.3±0.1 at 900 °C.

Keywords

Modulation-doping, Thermoelectrics, Nanocomposite, Silicon germanium (SiGe), Dimensionless figure-of-merit

The performance of thermoelectric materials depends on their dimensionless thermoelectric figure-of-merit $ZT = (S^2\sigma/\kappa)T$, where S is the Seebeck coefficient, σ the electrical conductivity, κ the thermal conductivity, and T the absolute temperature at which the properties are measured. The numerator $S^2\sigma$ is called the power factor[1]. It is generally recognized that for the next generation of thermoelectric materials, strategies to enhance the power factor[2-4] are essential in addition to those to decrease the thermal conductivity.

Silicon germanium (SiGe) alloys are suitable candidates for high temperature thermoelectric applications because of their reasonably good thermoelectric properties and superior long-term reliability at elevated temperatures. Consequently, SiGe thermoelectric modules with material ZT of 0.5 (p-type) and 0.9 (n-type) have been used in space radioisotope thermoelectric generators (RTGs) by US NASA since 1976[1]. New applications especially heat conversion at high temperatures demand higher ZTs for such materials applications. Recently, a good enhancement in ZT values has been demonstrated for both n- and p-type SiGe alloys by using a nanocomposite approach[5-8]. The lattice thermal conductivity of the nanocomposite samples is much lower compared to that of their equivalent large crystalline bulk materials because of the much increased grain boundaries of the numerous nanograins that effectively scatter long wavelength phonons. Using this approach, the peak ZT value of p-type nanostructured $Si_{80}Ge_{20}B_5$ samples was improved from 0.5 to 0.95[5], and that of n-type $Si_{80}Ge_{20}P_2$ from 0.93 to around 1.3[6]. However, these materials contain a fairly high concentration of Ge that is about a hundred times more expensive than Si. In 2009, Zhu $et\ al.$ reported[7] that by using the nanocomposite approach, only a 5% Ge replacement of Si is sufficient to further reduce the thermal conductivity of n-type nano-Si by a factor of 2, resulting in a ZT peak value of 0.94 in $Si_{95}Ge_5$ doped with GaP and P at ~900 °C, and this result is significant since a much smaller amount of expensive Ge is used. Furthermore, if Ge is entirely eliminated, the ZT peak of pure nano-Si would drop to about 0.7 at around 1000 °C[9]. Clearly there is a tradeoff between the cost and the performance of $Si_{1-x}Ge_x$ alloys.

Recently, we introduced a three dimensional (3-D) modulation-doping approach[10] to improve the power factor of thermoelectric nanocomposites by mainly increasing the mobility. Modulation-doping has been widely used in thin-film semiconductors that separate the charge carriers from the ionized dopants to reduce the charge scattering thus to increase the carrier mobility so to increase the electrical conductivity as a consequence[11-13]. The proposed modulation-doped sample is a two-phase nanocomposite made out of two different types of nanograins. Rather than uniformly dope the sample, dopants are incorporated into only one type of nanograins. Charge carriers spill over from the doped nanograins to the undoped or lightly doped matrix phase, leaving behind ionized nanograins. Instead of the usual heavy uniform doping in thermoelectric materials, causing strong ionized impurity scattering

of charges, ionized nanoparticles can be spatially placed much further apart in modulation-doping scheme, leading to reduced electron scattering for higher mobility. Traditionally, molecular beam epitaxy (MBE) was used to grow those thin layers, consisting of an undoped conducting layer (channel), a doped layer that donates carriers, and an undoped spacer layer separating the ionized dopants from the conducting channel. Adapting such a concept, our study[10] theoretically and experimentally demonstrated that modulation-doping is also effective in 3-D bulk nanocomposite systems by improving the mobility thus the power factor. The power factor of the p-type $Si_{86}Ge_{14}B_{1.5}$ uniform sample was improved by 40% using the modulation-doping approach, achieved by using a 30% fraction of $Si_{100}B_5$ nanograins in the intrinsic $Si_{80}Ge_{20}$ matrix to make a modulation-doped sample: $(Si_{80}Ge_{20})_{0.7}(Si_{100}B_5)_{0.3}$[10]. A smaller improvement of about 20% was observed in the power factor of n-type sample $(Si_{80}Ge_{20})_{0.8}(Si_{100}P_3)_{0.2}$ compared to its equivalent uniform nanocomposite $Si_{84}Ge_{16}P_{0.6}$[10]. However, the ZTs were not increased due to the high thermal conductivities of the nanoparticles of pure Si.

The modulation-doping scheme we reported produced enhancement in electrical conductivity leading to the increase in the electronic part of the thermal conductivity. Such increase in electronic part is inevitable because charge carriers are also heat carriers. At the same time, the increase in lattice part is also unavoidable since the nanoparticles Si have much higher thermal conductivity. Ideally, we want to maintain the low thermal conductivity of the nanostructured materials. Therefore modulation-doping scheme should be also focused on strategies to reduce the lattice part of the thermal conductivity. Here, we report our success on simultaneously improving the power factor and reducing the lattice part of the thermal conductivity by a new materials design and band alignment in the scheme of modulation-doping: using $Si_{95}Ge_5$ as the matrix (instead of $Si_{80}Ge_{20}$, lower Ge concentration not only increase the mobility but also reduce the cost) and $Si_{70}Ge_{30}P_3$ as the nanoparticles that has a much lower thermal conductivity, to eventually enhance the ZT.

Ideally, for modulation-doping in bulk nanocomposites, one wants to choose nanoparticles with a low density of states compared to the matrix. The nanoparticles should also form proper band alignments with the matrix to promote the flow of carriers from the nanoparticles into the matrix[14]. In this study, we have chosen $Si_{70}Ge_{30}P_3$ as the doped nanoparticles for two reasons: because of their good band alignment and their low thermal conductivity. It is known that SiGe and Si can form either type I or type II band alignment in thin-film heterostructures (Fig. 1)[13, 15]. In nanocomposites, it is difficult to determine the band alignment because such composites are obtained by consolidating two types of crystal grains into a bulk 3-D material instead of growing atomic layers one by one. Both types of grains might be under tension and the possible dangling bonds, impurities, and trapped charges at the

interfaces might all affect the final band alignment. For n-type materials, the nanoparticles should have relatively higher conduction band edges compared to the matrix grains to force the carriers to flow into the matrix. For our materials design, we accept type *II* band alignment which is the case for the Si/Ge interface[16] and therefore we chose nanoparticle grains containing more Ge compared to the matrix. From our experimental observations, which will be shown later, one can conclude that the band discontinuity in our case is type *II* and is large enough for the purpose of modulation-doping. Moreover, a larger density of states effective mass (mainly due to the larger valley degeneracy of Si compared to Ge) in the Si rich matrix ($Si_{95}Ge_5$) compared to the selected nanoparticles leads to more available energy states for the carriers to fill.

For the consideration of the thermal conductivity, $Si_{70}Ge_{30}$ has the lowest thermal conductivity among $Si_{1-x}Ge_x$ alloys[17]. Using $Si_{70}Ge_{30}P_3$ composition as the nanoparticles then has clearly a big advantage in our experiment: as we increase the nanoparticle molar fraction, the thermal conductivity decreases and the electrical conductivity increases simultaneously.

The alloyed $Si_{1-x}Ge_x$ nanopowders were prepared by ball milling pure elements of Si, Ge, and P for about 10 hours in a high energy ball mill. Then they were mixed in the container according to the designed molar ratio for a very short time (several minutes). Finally the powder mixtures were consolidated rapidly into 12.7 mm disks in a graphite die by a dc hot press method. The sample density was measured by the Archimedean method and all samples reported here have densities close to the theoretical values (Table 1). We measured the electrical conductivity and the Seebeck coefficient using a commercial four-probe system (ULVAC, ZEM-3) and using 2 mm × 2 mm × 12 mm bars cut from the disks. The thermal diffusivity was measured directly on these disks by laser flash (NETZSCH LFA 457) and the specific heat was measured by differential scanning calorimetry (DSC, NETZSCH 200-F3). All experiments were repeated a few times and the data are within the measurement errors (3% for electrical conductivity, thermal diffusivity, specific heat, 4% for thermal conductivity, 5% for Seebeck coefficient, resulting in an uncertainty of 11% for the *ZT* values). Room temperature Hall measurements were performed on polished thin bulk samples using a Physical Properties Measurement System (PPMS) from Quantum Design with typical sample dimensions of 0.5 mm x 2 mm x 11 mm. The hot-pressed samples were also cut, polished, and then ion-milled for microstructure study using Transmission Electron Microscope (TEM, JEOL JSM2010F) techniques.

We study the thermoelectric properties of the proposed modulation-doped $(Si_{95}Ge_5)_{1-x}(Si_{70}Ge_{30}P_3)_x$ as a function of nanoparticle molar fraction, *x*. For comparison purposes, we also prepared composition equivalent uniform samples as references: $Si_{93.75}Ge_{6.25}P_{0.15}$, $Si_{91.25}Ge_{8.75}P_{0.45}$,

$Si_{88.75}Ge_{11.25}P_{0.75}$, $Si_{86.25}Ge_{13.75}P_{1.05}$, and $Si_{83.75}Ge_{16.25}P_{1.35}$. Figure 2a shows the electrical conductivity at room temperature as a function of Ge concentration. In modulation-doped samples, a fairly good electrical conductivity σ of 9.25×10^4 Sm^{-1} is achieved with even only 5% nanoparticles and σ continues to rise with increasing nanoparticle ratio. When we increase the molar fraction of nanoparticles, more carriers are introduced into the matrix to increase the electrical conductivity through modulation-doping. However, at the same time, these nanoparticles also introduce excessive interfaces and a larger static potential barrier (when compared to ionized impurity atoms) to scatter the electrons, which negatively affect the electrical conductivity. So when the nanoparticle molar fraction increases to more than 35%, the electrical conductivity starts to decrease as shown in Fig. 2a. Similar trends are observed in the equivalent samples. However, for the equivalent samples, the electrical conductivity starts to decrease at lower Ge molar fractions and the peak value of the electrical conductivity in this series of samples is much lower than that of the modulation-doped samples. When the nanoparticle molar fraction is 35%, the electrical conductivity of the modulation-doped sample has the highest value of 1.63×10^5 Sm^{-1} (54% higher compared to the corresponding equivalent uniform composition $Si_{86.25}Ge_{13.75}P_{1.05}$). This electrical conductivity value is also much higher than that of our previously reported data[10] with a similar composition, indicating that the current materials design is more favorable for n-type $Si_{1-x}Ge_x$ samples. We should point out that the mobility of our best sample with 35% nanoparticles at room temperature is 36.42 $cm^2V^{-1}s^{-1}$ which is much higher compared to its uniform counterpart $Si_{86.25}Ge_{13.75}P_{1.05}$ with a mobility of 24.26 $cm^2V^{-1}s^{-1}$, while the carrier concentration stays almost the same at around 2.78×10^{20} cm^{-3} in both samples. Surprisingly, the mobility of the modulation-doped samples is also higher than that (29.21 $cm^2V^{-1}s^{-1}$) of the uniform nanocomposite $Si_{95}Ge_5P_2$ (optimally doped matrix) that has much less Ge, further proving the advantage of our current materials designing approach.

For the thermal conductivity κ (Fig. 2b), unlike our previous study[10] in which the thermal conductivity increased largely with the addition of nanoparticles (pure Si was used), here, it is natural that κ rapidly goes down as the ratio of nanoparticles increases since the doped nanoparticles are less thermally conductive than the matrix. The lowest room temperature thermal conductivity reaches about 3.90 $Wm^{-1}K^{-1}$ at the highest nanoparticle molar ratio (45%), equivalent to a composition of $Si_{83.75}Ge_{16.25}P_{1.35}$. Comparing to the equivalent uniform sample, modulation-doped samples have higher electronic thermal conductivities because of their higher electrical conductivities. For example for the 45% volume fraction of nanoparticles, the electronic part of the thermal conductivity is around 1 $Wm^{-1}K^{-1}$ using the Wiedemann Franz law assuming a Lorenz number of 2.44×10^{-8} $W\Omega K^{-2}$, while that of the equivalent sample is only 0.7 $Wm^{-1}K^{-1}$. In this study, we were able to maintain the total thermal

conductivity of the modulation-doped sample as low as those of the single-phase equivalent samples, which means that the lattice part of the thermal conductivity in our modulation-doped nanocomposite sample is lower than its equivalent single-phase sample.

Figure 2c shows the ratio σ/κ (at room temperature) dependence of the Ge concentration. It is clearly shown that the σ/κ ratio of the modulation-doped samples increases much faster than those of the equivalent uniform samples with increasing Ge content. In fact, most of the rapid increase in σ/κ is from the rapid increase in the electrical conductivity (Fig. 2a), while the values of the thermal conductivities (Fig. 2b) are comparable, which is very different from the situation when pure Si was used as the nanoparticle material. The highest σ/κ value for our modulation-doped samples happens at 35% nanoparticles, or 13.75% Ge equivalently, which is 54% higher than the σ/κ of its equivalent uniform nanocomposite $Si_{86.25}Ge_{13.75}P_{1.05}$.

Figure 3 shows the temperature dependence of the thermoelectric properties of modulation-doped samples. This figure shows that the increase of the electrical conductivity (Fig. 3a) decreases the Seebeck coefficient (Fig. 3b) due to the usual interdependence of the transport parameters[18-20]. The obvious trend of the lower thermal diffusivity (Fig. 3c) and thermal conductivity (Fig. 3e) is caused by the interface phonon scattering due to the presence of more nanoparticles. The low thermal conductivity also benefits from the low specific heat (Fig. 3d) of the nanoparticles. With 35% nanoparticles, our modulation-doped sample has the biggest advantage on the σ/κ value over its equivalent uniform sample (Fig. 2c) and the highest ZT value reaches 1.3 at 900 °C (Fig. 3f), about the same as that of the best uniform nanocomposite $Si_{80}Ge_{20}P_2$ reported for $Si_{1-x}Gex$ so far[6], but less Ge is used in the modulation-doped samples, meaning lower cost.

Figure 4 shows the comparison for each individual property between the best modulation-doped sample $(Si_{95}Ge_5)_{0.65}(Si_{70}Ge_{30}P_3)_{0.35}$ and its equivalent uniform sample $Si_{86.25}Ge_{13.75}P_{1.05}$. To compare the modulation-doping with uniform impurity doping, we also include the data for the optimally doped matrix, $Si_{95}Ge_5P_2$. As one could see, over the whole temperature range, the modulation-doped sample has a higher electrical conductivity due to higher carrier mobility than the equivalent uniform sample (Fig. 4a). The difference is pretty large at low temperature but gets smaller as the temperature increases, since electron-phonon scattering increases with temperature and starts to dominate at high temperatures[1]. Another possibility is that the interfaces may also have a larger impact on carrier transport at high temperatures. Compared to the modulation-doped sample, the uniform $Si_{95}Ge_5P_2$ sample has a much higher carrier concentration of 4.01×10^{20} cm^{-3} at room temperature due to its higher P concentration, which should be the reason for its higher electrical conductivity even though its carrier

mobility is lower. The modulation-doped sample has a similar thermal diffusivity (Fig. 4d) and a similar specific heat (C_p) values (Fig. 4e) compared to the equivalent uniform sample. As a result, the thermal conductivity (Fig. 4f) of the modulation-doped sample is similar to that of the equivalent uniform sample. However the temperature dependence of σ/κ (Fig. 4g), clearly shows that the modulation-doped sample has an advantage over the whole temperature range. It is important to note that the Seebeck coefficient of any modulation-doped sample in our study is similar to that of its corresponding equivalent uniform sample, similar to our observations in the previous report[10]. For example in Fig. 4b, considering the 5% experimental error bar, the values for Seebeck coefficient are very close over the whole temperature range. Overall, our modulation-doping approach has improved the value of σ/κ, but has left the Seebeck coefficient almost untouched. With higher electrical conductivity and a similar Seebeck coefficient, the modulation-doped sample shows an improved power factor compared to its equivalent uniform sample, leading to the fact that the modulation-doped sample shows better ZT values (Fig. 4h) than the equivalent uniform sample. Because the absolute ZT value at low temperature is small, one may find the difference at low temperature insignificant. Actually, the improvement at room temperature is 23%. At 900 °C, the peak value is close to 1.3, about 30% higher than the equivalent uniform sample ($ZT \sim 1.0$) and 36% higher than the optimally doped matrix ($ZT \sim 0.9$). Comparing to the previously reported best n-type alloy $Si_{80}Ge_{20}P_2$,[6] the peak ZTs are basically the same but the modulation-doped samples contain much less Ge: equivalent to $Si_{86.25}Ge_{13.75}P_{1.05}$, meaning a much lower fabrication cost.

Since the matrix and nanoparticles have a different Si to Ge ratio, they may diffuse into each other during the hot-pressing process. To prove whether such diffusion has really happened, we performed an energy dispersive spectroscopy (EDS) study on our hot-pressed modulation-doped samples using a transmission electron microscope (TEM). For reference purposes, $Si_{95}Ge_5$ nanopowders were measured first. The EDS data repeatedly showed that the average atomic ratio between Si and Ge is 94.3:5.7 which is very close to the as-prepared composition (95:5). After the validation step, we then measured the best modulation-doped samples with a 35% nanoparticle molar fraction. At low magnifications (30,000-100,000) with the incident beam spread over a larger sample area, EDS results showed that the average chemical composition of the area is $Si_{86}Ge_{14}$, consistent with the designed equivalent composition $Si_{86.25}Ge_{13.75}$. At higher magnification (Fig. 5a and 5b), we found that there are two typical domains with different compositions. The ones with more Si (Fig. 5a), with the measured Si:Ge at five positions to be 89.1:10.9 (A), 89.3:10.7 (B), 89.4:10.6 (C), 89.3:10.7 (D), and 90.9:9.1 (E), give an average value of 89.6:10.4, which indicates 5% diffusion of Ge from nanoparticles into the matrix when compared to the original matrix composition of 95:5. The other domains turn out to have

higher Ge (Fig. 5b): 73.1:26.9 (A), 69.3:30.7 (B), 75.1:24.9 (C), and 75.1:24.9 (D), giving an averaging 73.1:26.9, little bit higher Si than that of the nanoparticles $Si_{70}Ge_{30}P_3$, a result of the minor diffusion. Typical EDS spectra for each case are given in Fig. 5c. From these results, we could say that even though there might be some diffusion between the matrix and the nanoparticles, the two components still keep apart from each other. Compared to a thin-film configuration of modulation-doped structures, a better design will be to have a spacer layer. The spacer would have a dual role. First it will prevent grain growth; second, it will separate the carriers from their parent atoms. The spacer itself should not react with either the host or the nanoparticles. In n-type configuration, the case of this study, the spacer band should align below the nanoparticles` band and above the host matrix, so that the carriers can fall from the nanoparticles to the spacer and then to the matrix. However, how to make those spacer layers turns out to be extremely challenging in nanocomposites. Nevertheless, modulation-doping behavior is successfully demonstrated in this work.

In conclusion, we designed a new materials approach to unambiguously demonstrate the effectiveness of modulation-doping in thermoelectric nanocomposites. The electrical conductivity of a $Si_{86.25}Ge_{13.75}P_{1.05}$ sample was improved by 54% using the modulation-doping approach in $(Si_{95}Ge_5)_{0.65}(Si_{70}Ge_{30}P_3)_{0.35}$ that has the same overall composition. The enhancement was due to the 50% enhancement of the carrier mobility by spatially separating carriers from their parent atoms. More importantly, the thermal conductivity was kept low due to the low thermal conductivity of the nanoparticles. In fact the two-phase composite has a lower lattice thermal conductivity compared to its equivalent single phase nanocomposite. At the same time, the Seebeck coefficient was not deteriorated. The unaffected Seebeck coefficient, combining with the enhanced electrical conductivity and the lower thermal conductivity produces a peak *ZT* of ~1.3 at 900 °C. The resulted *ZT* is about 30-40% higher than the equivalent uniform sample and the optimally doped matrix, and could already compete with the state-of-the-art n-type $Si_{80}Ge_{20}P_2$ thermoelectric bulk materials with a much lower materials cost. To further improve the modulation-doping approach, using a thin spacer layer to minimize the diffusion would be expected to further improve the measured performance.

Table 1 Theoretical and measured densities of as-prepared silicon germanium nanocomposite samples.

Sample Type	Modulation Doped (NPs molar fraction)					Equivalent Uniform					Uniform $Si_{95}Ge_5P_2$
	5%	15%	25%	35%	45%	5%	15%	25%	35%	45%	
Theoretical (gcm^{-3})	2.517	2.592	2.666	2.741	2.816	2.517	2.592	2.666	2.741	2.816	2.480
Measured (gcm^{-3})	2.505	2.596	2.662	2.731	2.813	2.511	2.590	2.671	2.728	2.815	2.482
Percentage (%)	99.5	100.2	99.8	99.6	99.9	99.8	99.9	100.2	99.5	100.0	100.1

Figure captions

Figure 1 Type *I* (strained SiGe on Si) and type *II* (strained Si on SiGe) band alignments.

Figure 2 (a) Electrical conductivity σ, **(b)** thermal conductivity κ, and **(c)** σ/κ ratio of modulation-doped $Si_{1-x}Ge_x$ nanocomposite samples as a function of Ge concentration, in comparison with those of equivalent uniform compositions.

Figure 3 Temperature dependence of **(a)** electrical conductivity σ, **(b)** Seebeck coefficient *S*, **(c)** diffusivity, **(d)** specific heat C_p, **(e)** thermal conductivity κ, and **(f)** *ZT* of modulation-doped $Si_{1-x}Ge_x$ nanocomposite samples with different nanoparticle molar fractions.

Figure 4 Temperature dependent **(a)** electrical conductivity σ, **(b)** Seebeck coefficient *S*, **(c)** power factor, **(d)** diffusivity, **(e)** specific heat C_p, **(f)** thermal conductivity κ, **(g)** σ/κ ratio, and **(h)** *ZT* of modulation-doped $Si_{1-x}Ge_x$ nanocomposite sample with a 35% nanoparticle molar fraction, in comparison with those of equivalent uniform $Si_{86.25}Ge_{13.75}P_{1.05}$ and optimally-doped $Si_{95}Ge_5P_2$ uniform samples.

Figure 5 (a-b) TEM images, and **(c)** EDS spectra [the spectrum in **(c)** is for the grain E in **(a)**, the inset in **(c)** is for the grain A in **(b)**] of modulation-doped sample with a 35% nanoparticle molar fraction.
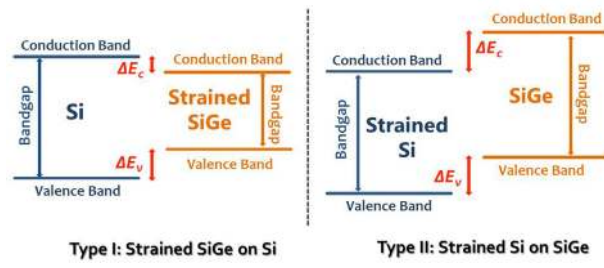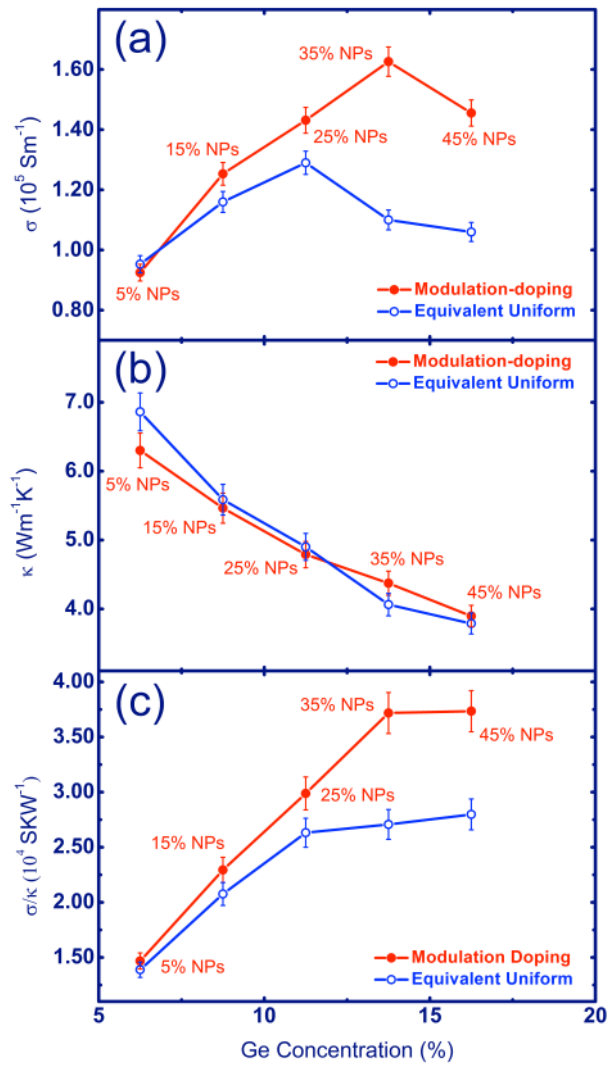
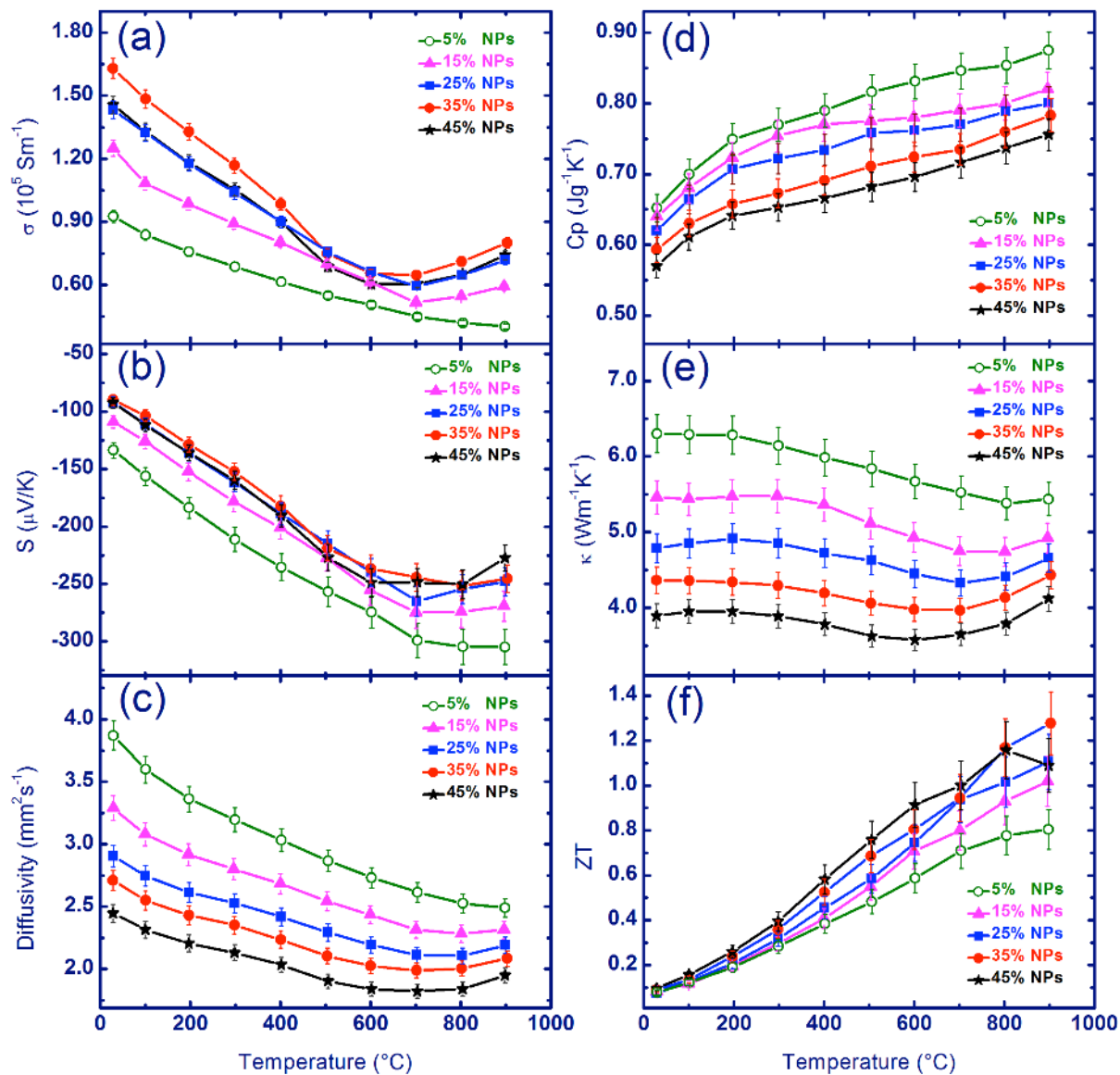**Figure 1 Bo Yu *et al.***

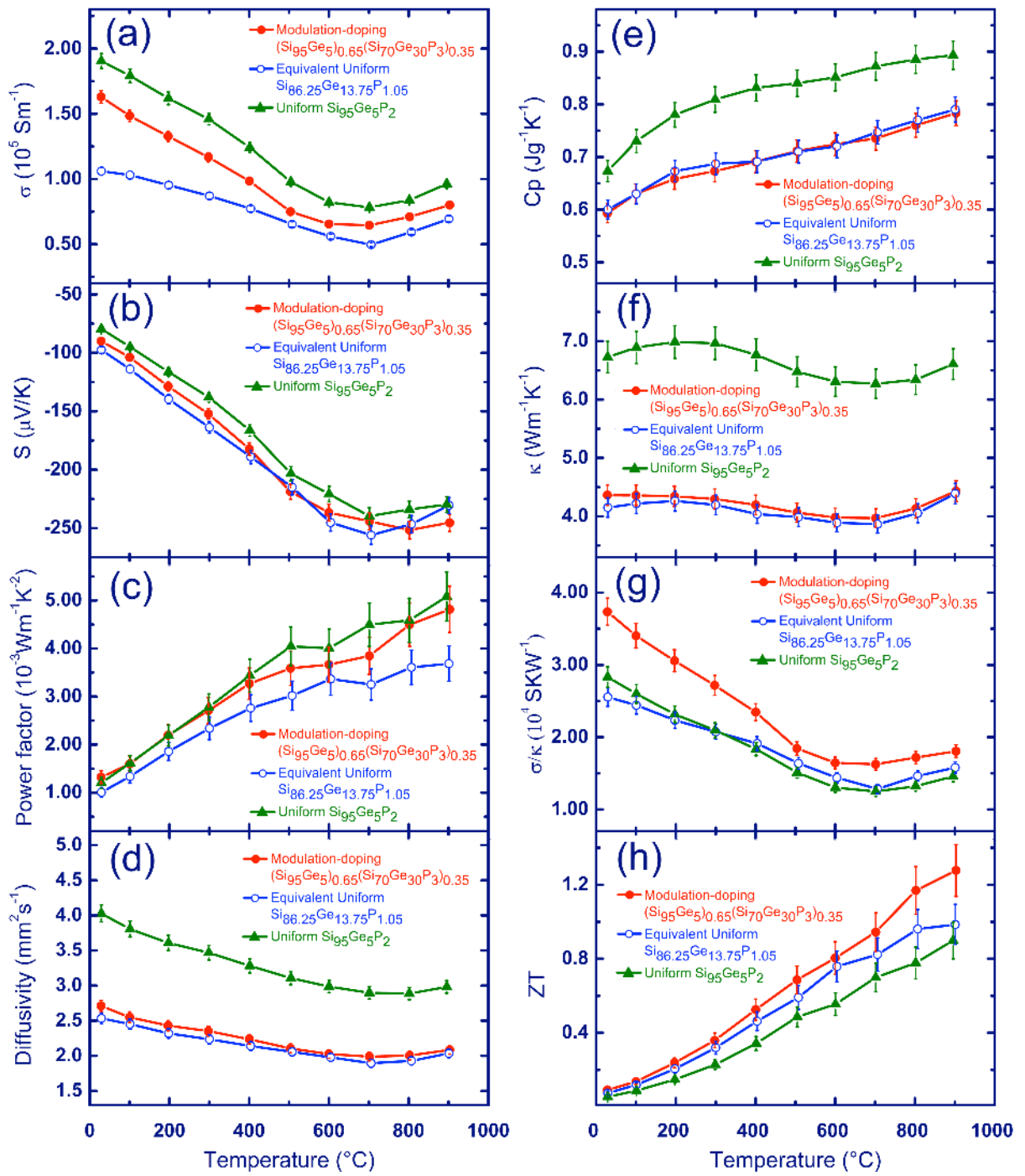**Figure 2 Bo Yu *et al.***

Figure 3 Bo Yu *et al.*
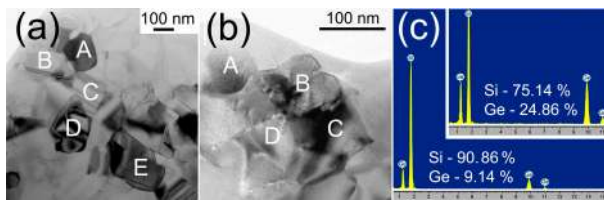
Figure 4 Bo Yu *et al.*

Figure 5 Bo Yu *et al.*

References

(1) Rowe, D. M. *CRC Handbook of Thermoelectrics*; CRC Press: Boca Raton, FL, 1995

(2) Mahan, G. D.; Sofo, J. O. *Proc. Natl. Acad. Sci. USA* **1996**, *93*, 7436

(3) Heremans, J. P.; Thrush, C. M.; Morelli, D. T.; Wu, M. C. *Phys. Rev. Lett*. **2002**, *88*, 216801

(4) Zebarjadi, M.; Esfarjani, K.; Bian, Z. X.; Shakouri, A. *Nano Lett*. **2011**, *11*, 225

(5) Joshi, G.; Lee, H.; Lan, Y. C.; Wang, X. W.; Zhu, G. H.; Wang, D. Z.; Muto, A. J.; Tang, M. Y.; Song, J. K. S.; Dresselhaus, M. S.; Chen, G.; Ren, Z. F. *Nano Lett*. **2008**, *8*, 4670

(6) Wang, X. W.; Lee, H.; Lan, Y. C.; Zhu, G. H.; Joshi, G.; Wang, D. Z.; Yang, J.; Muto, A. J.; Tang, M. Y.; Song, J. K. S.; Dresselhaus, M. S.; Chen, G.; Ren, Z. F. *Appl. Phys. Lett*. **2008**, *93*, 193121

(7) Zhu, G. H.; Lee, H.; Lan, Y. C.; Wang, X. W.; Joshi, G.; Wang, D. Z.; Yang, J.; Vashaee, D.; Guilbert, H.; Pillitteri, A.; Dresselhaus, M. S.; Chen, G.; Ren, Z. F. *Phys. Rev. Lett*. **2009**, *102*, 196803

(8) Lan, Y. C.; Minnich, A. J.; Chen, G.; Ren, Z. F. *Adv. Funct. Mater*. **2010**, *20*, 357

(9) Bux, S. K.; Blair, R. G.; Gogna, P. K.; Lee, H.; Chen, G.; Dresselhaus, M. S.; Kaner, R. B.; Fleurial, J. -P. *Adv. Funct. Mater*. **2009**, *19*, 2445

(10) Zebarjadi, M; Joshi, G.; Zhu, G. H.; Yu, B.; Minnich, A. J.; Lan, Y. C.; Wang, X. W.; Dresselhaus, M. S.; Ren, Z. F.; Chen, G. *Nano Lett*. **2011**, *11*, 2225

(11) Dingle, R.; Störmer, H. L.; Gossard, A. C.; Wiegmann, W. *Appl. Phys. Lett*. **1978**, *33*, 665

(12) Daembkes, H. *Modulation-doped Field-effect Transistors: Principles, Design, and Technology*, 2nd ed.; IEEE Press: New York, 1991

(13) Schäffler, F. *Semicond. Sci. Technol*. **1997**, *12*, 1515

(14) Zebarjadi, M.; Esfarjani, K.; Dresselhaus, M. S.; Ren, Z. F.; Chen, G. *Energy Environ. Sci*. **2012**, *5*, 5147

(15) Yang, L. F.; Watling, J. R.; Wilkins, R. C. W.; Boriçi, M.; Barker, J. R.; Asenov, A.; Roy, S. *Semicond. Sci. Technol*. **2004**, *19*, 1174

(16) Van de Walle, C. G.; Martin, R. M. *Phys. Rev. B*. **1986**, *34*, 5621

(17) Stohr, J.; Klemm, W. *Z. Anorg. Allegem. Chem*. **1954**, *241*, 305

(18) Snyder, G. J.; Toberer, E. S. *Nat. Mater*. **2008**, *7*, 105

(19) Dresselhaus, M. S.; Chen, G.; Tang, M. Y.; Yang, R. G.; Lee, H.; Wang, D. Z.; Ren, Z. F.; Fleurial, J. -P.; Gogna, P. *Adv. Mater*. **2007**, *19*, 1043

(20) Minnich, A. J.; Dresselhaus, M. S.; Ren, Z. F.; Chen, G. *Energy Environ. Sci*. **2009**, *2*, 466